Retrofit and Repair of Reinforced Concrete Columns with Active Confinement

J. Rincón & S. Pujol
University of Canterbury, Department of Civil and Natural Resources Engineering, Christchurch.

ABSTRACT

Popular retrofit techniques such as steel and concrete jacketing, and fibre-reinforced polymer wrapping have been proven to be effective in increasing shear strength and improving drift capacity of RC columns. Nevertheless, those techniques are labour-intensive and have involved installation procedures. Ease of installation is also key when it comes to emergency repairs needed after strong ground motion. After a strong earthquake, the repair of a structure must be done quickly to ensure rapid restoration of the safety of occupants and neighbours. An easy-to-design and easy-to-implement retrofit technique involving post-tensioned external clamps fastened around the column is examined here. The post-tensioned clamps consist of four corner brackets made with pairs of steel angles and threaded rods connecting the brackets to each other. The confining lateral pressure provided by the clamps is expected to help delay the spalling and crushing of concrete as well as the formation of inclined shear cracks. Results of tests on full-scale RC columns furnished with the proposed clamps suggest the clamps can be effective in increasing column shear strength and drift capacity.

1 INTRODUCTION

Reinforced concrete structures, designed and constructed before to the introduction of seismic detailing provisions in the 1970s, typically include non-ductile RC columns. Those are columns with insufficient transverse reinforcement, inadequate lap splices, and/or deficient steel detailing. Such columns have been observed to fail during strong earthquakes (Hanson & Degenkolb, 1969; Lew & Leyendecker, 1971; Tillotson, 1960). Confinement of the concrete core is a well-known and effective method of obtaining ductile behaviour (Kent & Park, 1971; Mander et al., 1988b, 1988a; Richart et al., 1928; Roy & Sozen, 1965). Although steel jacketing and FRP wrapping have been proven to be successful in improving ductility of RC columns, those techniques have been also reported as being labour-intensive and expensive for mass retrofit of large inventory of structures (Aboutaha et al., 1999; Burgoyne & Balafas, 2007; Raza et al., 2019; Rodriguez & Park, 1994). In addition, similar to conventional ties, steel jackets and FRP wraps require formation of cracks and expansion of the concrete core to be 'activated'. In that sense, the confinement is 'passive'. 'Active' confinement, by contrast, can provide lateral confining pressure before the formation of the mentioned cracking and expansion that inevitably relate to perceived damage.

Relative to conventional ‘passive’ confinement, much less work has been done on the idea of active confinement. Some investigations (Gamble et al., 1996; Saatcioglu & Yalcin, 2003; Yamakawa et al., 2000) have been focused on the use of high-strength steel to apply lateral pre-tensioning. Others (Kyoda et al., 2011; Yamakawa et al., 2005) have studied the implementation of prestressed FRP belts, while others have explored the use of shape memory alloys (SMAs) (Andrawes & Shin, 2009; Choi et al., 2008; Shin & Andrawes, 2014; Tran et al., 2015). Results from such investigations suggested that active confinement improved axial-carrying capacity, shear strength, and ductility of the confined concrete more effectively than passive confinement (Holmes et al., 2015; Moghaddam et al., 2010; Rousakis & Tourtouras, 2014). Despite positive results, active confinement using traditional procedures possess practical constrains, making it less common than passive FRP and steel jacketing confinement.

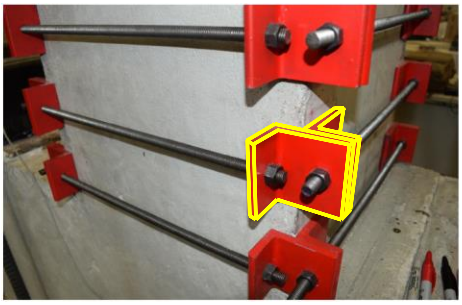

Figure 1: Clamps design (Skillen, 2020)

In an attempt to ease procedures to produce active confinement, Skillen proposed simpler post-tensioning clamps consisting of steel angles and high-strength threaded rods as shown in Figure 1 (Skillen, 2020). Skillen’s test results suggested again that shear resistance and drift capacity of columns vulnerable to shear can be dramatically improved with post-tensioned transverse reinforcement.

2 EXPERIMENTAL WORK

Ongoing research on the effects of active confinement on column drift capacity includes tests on 11 large-scale RC columns. Here, results from six of those 11 RC columns are presented: columns C3, C5, C6, C9, C10, and C11. Test columns were subjected to displacement reversals and approximately constant axial loads ($0.15A_g f'_c$). The axial load was controlled with a manual pump, equipped with a pressure indicator and a release valve.

With exception of C11, columns had no conventional internal ties. Columns C3, C5, C6, and C9 were used to test the post-tensioned clamps as a retrofit measure, while C10 and C11 were used to explore the feasibility of the clamps as a repair measure. Table 1 shows key tests details and measured material properties.

Table 1: Summary of measured material properties.

Specimen	Test	f'_c (MPa)	f_y (MPa)	f_u (MPa)	f_{pty} (MPa)	f_{ptu} (MPa)	Internal ties?	f_{ty} (MPa)	f_{tu} (MPa)
C3	Retrofit	30	555	698	820	922	No	-	-
C9	Retrofit	23	518	647	820	922	No	-	-
C5	Retrofit	36	555	698	820	922	No	-	-
C6	Retrofit	24	555	698	820	922	No	-	-
C10	Repair	23	518	647	820	922	No	-	-
C11	Repair	23	518	647	820	922	Yes	550	680

f'_c: Concrete cylinder compressive strength; f_y: longitudinal reinforcement yield stress; f_u: longitudinal reinforcement ultimate stress; f_{pty}: Post-tensioning transverse reinforcement yield stress; f_{ptu}: Post-tensioning transverse reinforcement ultimate stress; f_{ty}:

Conventional transverse reinforcement yield stress; f_{tu}: Conventional transverse reinforcement ultimate stress. Each of the measured material properties corresponds to the average of results from three coupons.

Figure 2 shows the test setup and key details of the test columns. The clamps used were similar to those used by Skillen (2020) (Fig. 1). They were designed using Equation 1 (Richart, 1927). The nominal resistance to shear v_n is expressed as the contribution to shear attributed to the concrete v_c and the contribution attributed to the transverse reinforcement v_s. Equation 1 can be rewritten as Equation 1a.

$$v_n = v_c + v_s \tag{1}$$

$$v_n = v_c + r_{pt} \cdot f_{pty} \tag{1a}$$

$$r_{pt} = \frac{A_{pt}}{b \cdot s_{pt}} \tag{2}$$

where r_{pt} = post-tensioned transverse reinforcement area ratio, calculated using Equation 2; f_{pty} = yield stress of the post-tensioned transverse reinforcement; A_{pt} = total cross-sectional area of post-tensioned transverse reinforcement within spacing s_{pt}; b = width of column cross section; s_{pt} = spacing of post-tensioned transverse reinforcement.

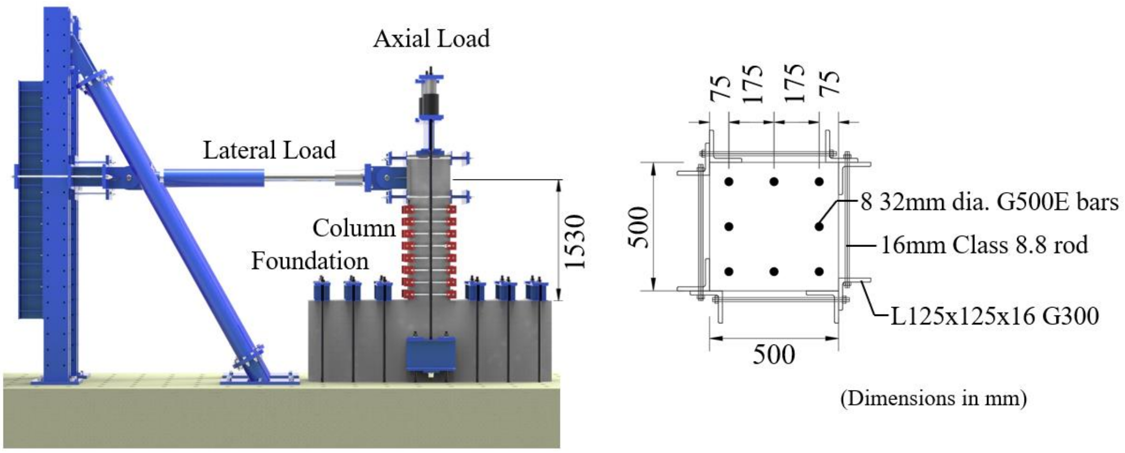

Figure 2: Test setup and specimen's details

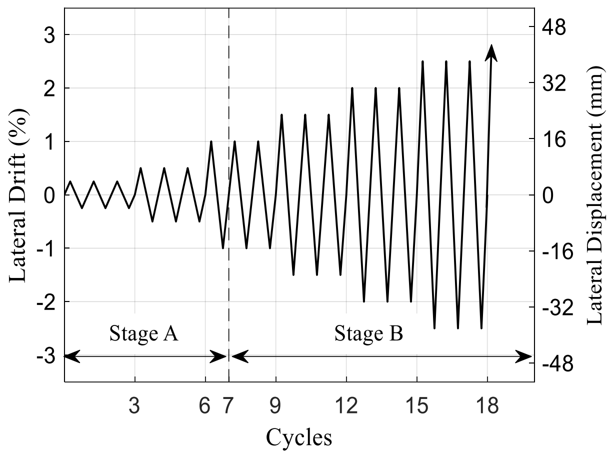

Figure 3: Loading protocol

Figure 3 shows the loading protocol. The columns were subjected to three lateral cycles at every target drift ratio until the lateral-load carrying capacity decreased by more than 50% of the maximum reached at any previous cycle.

Columns C10 and C11, which were used to test the clamps as repair measure, were loaded in two stages, A and B. Stage A consisted in applying three cycles at 0.25% drift and 0.5% drift, and the first cycle at 1% drift. The intent of Stage A was to cause initial damage represented in flexural and shear cracks. Columns had no post-tensioned clamps during stage A. After initial damage, the columns were repaired by furnishing them with clamps. Then, stage B of the loading protocol was applied until end of test.

3 TEST RESULTS AND DISCUSSION

3.1 As a retrofit measure

The effects of the initial clamp prestress on the shear strength and drift capacity of RC columns were studied by comparing columns with low initial clamp prestress with columns with high initial clamp prestress. Average lateral pressure σ_L is assumed to be proportional to the post-tensioned transverse reinforcement area ratio r_{pt} and the initial prestress in the clamps f_{pti} as shown in Equation 3.

$$\sigma_L = r_{pt} \cdot f_{pti} \tag{3}$$

C3 and C9 were furnished with four clamps spaced at 300 mm ($r_{pt} = 0.21\%$), whereas columns C5 and C6 had six clamps spaced at 200 mm ($r_{pt} = 0.32\%$). C3 and C5 had clamps with low prestress f_{pti} ($0.1f_{pty}$), whereas C9 and C6 had clamps with high prestress f_{pti} ($0.7f_{pty}$). Table 2 summarises key test variables and results. Two values of the maximum measured shear force (V_{max}) are given, which correspond to the pushing (positive) and pulling (negative) directions, but only the mean drift capacity is shown. Drift capacity is defined here as the drift that the column reaches before its lateral-load resistance drops to 80% of the maximum measured load.

Table 2: Summary of test results on retrofitted columns

Specimen	r_{tr} (%)	s_{pt} (mm)	s_{pt}/d	r_{pt} (%)	f_{pti} (MPa)	σ_L (MPa)	V_{max} (kN)	*D.C. (%)*
C3	0	300	0.7	0.21	$0.1f_{pty}$	0.2	+450/-480	3.0
C9	0	300	0.7	0.21	$0.7f_{pty}$	1.1	+530/-540	4.0
C5	0	200	0.5	0.32	$0.1f_{pty}$	0.3	+570/-550	5.5
C6	0	200	0.5	0.32	$0.7f_{pty}$	1.7	+530/-540	5.1

r_{tr}: reinforcement ratio of conventional ties; s_{pt}: spacing of post-tensioned clamps; *d:* effective depth ratio; r_{pt}: reinforcement ratio of post-tensioned clamps; f_{pti}: initial prestress in the clamps; σ_L: lateral confining stress on the column caused by the clamps; V_{max}: maximum measured shear force; *D.C.*: Drift Capacity.

3.1.1 Column C3 vs Column C9

Figure 4a shows the hysteretic response of columns C3 and C9. The expected maximum lateral load V_p during the test was 510 kN and the associated unit plastic shear stress v_p was 2.4 MPa. The maximum measured lateral load resisted by C3 ($\sigma_L = 0.2$ MPa or $0.04\sqrt{f'_c}$) was 480kN and the associated unit shear stress v_{max} was 2.3 MPa or $0.41\sqrt{f'_c}$. It is inferred that C3 did not reach flexural yielding of the longitudinal reinforcement and the mode of failure was driven by a gradual disintegration of the concrete core (Figure 4b). The drift capacity of C3 was 3.0%.

Compared with C3, column C9 ($\sigma_L = 1.1$ MPa or $0.23\sqrt{f'_c}$) had a drift capacity of 4% and a more stable response. C9 resisted a maximum applied lateral force of 540 kN ($v_{max} = 2.5$ MPa or $0.53\sqrt{f'_c}$). C9 not only reached flexural yielding of the longitudinal reinforcement (at a drift ratio close to 1.5%), but its response post-yielding was more ductile than C3. Before failure, fewer and narrower cracks were observed in C9 than in C3 (Figure 4c). Lateral prestress caused by the clamps on C9 precluded the formation of large, inclined shear cracks observed in C3. In addition, the lateral prestress increased the drift capacity from 3% (C3) to 4% (C9), which is a relative increase of 33%.

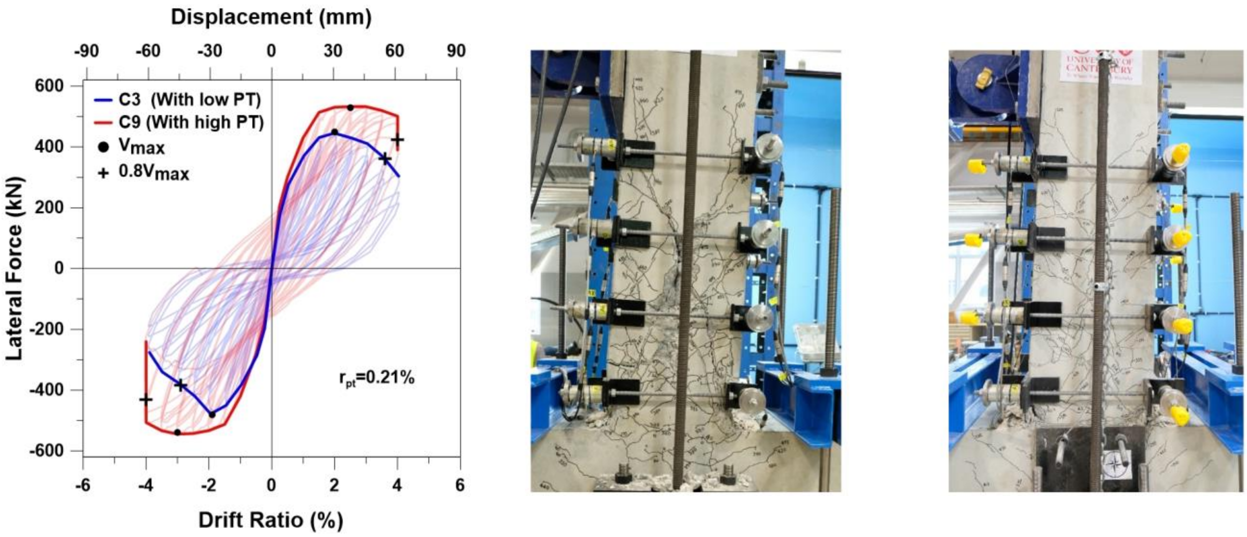

a) *b)* *c)*

Figure 4: a) Hysteretic response of columns C3 and C9; b) Column C3 at a drift ratio of 3.5%; c) Column C9 at a drift ratio of 3.5%

3.1.2 Column C5 vs Column C6

The measured hysteretic responses of columns C5 ($\sigma_L = 0.3$ MPa or $0.05\sqrt{f'_c}$) and C6 ($\sigma_L = 1.7$ MPa or $0.35\sqrt{f'_c}$) are shown in Figure 5a. Both columns reached flexural yielding at a drift ratio of 1.5%, approximately. The maximum measured shear force resisted by C5 was 570 kN ($v_{max} = 2.7$ MPa or $0.45\sqrt{f'_c}$). The drift capacity of C5 was 5.5%. Column C6 resisted a maximum applied lateral force of 540 kN ($v_{max} = 2.5$ MPa or $0.51\sqrt{f'_c}$). The drift capacity of C6 was 5.0%.

Column C5 maintained its lateral resistance during the first cycle at a drift of 5.5%. Nevertheless, a large inclined crack, spanning from the second clamp (from bottom) to the base of the column, caused a rapid disintegration of the concrete core. In the third cycle at a drift ratio of 5.5%, the column slid along the mentioned crack, triggering an abrupt loss of the lateral-carrying capacity.

Reaching a drift capacity of 5%, Column C6 failed in a mechanism controlled by flexure rather than by shear. Fewer cracks were observed in this test unit than in C5 (Figure 5b). For C6, severe deterioration of the concrete was observed in the compression zones (Figure 5c). It is plausible that this deterioration (that was not as clear in C5) was related to the weaker concrete strength of C6. C5 had f'_c = 36 MPa, whereas C6 had f'_c = 24 MPa. Differences in f'_c occurred because 1) the quality control at the mixing plant did not allow for more uniform values of f'_c, and 2) the specimens were cast from different concrete batches reportedly made using the same mix design.

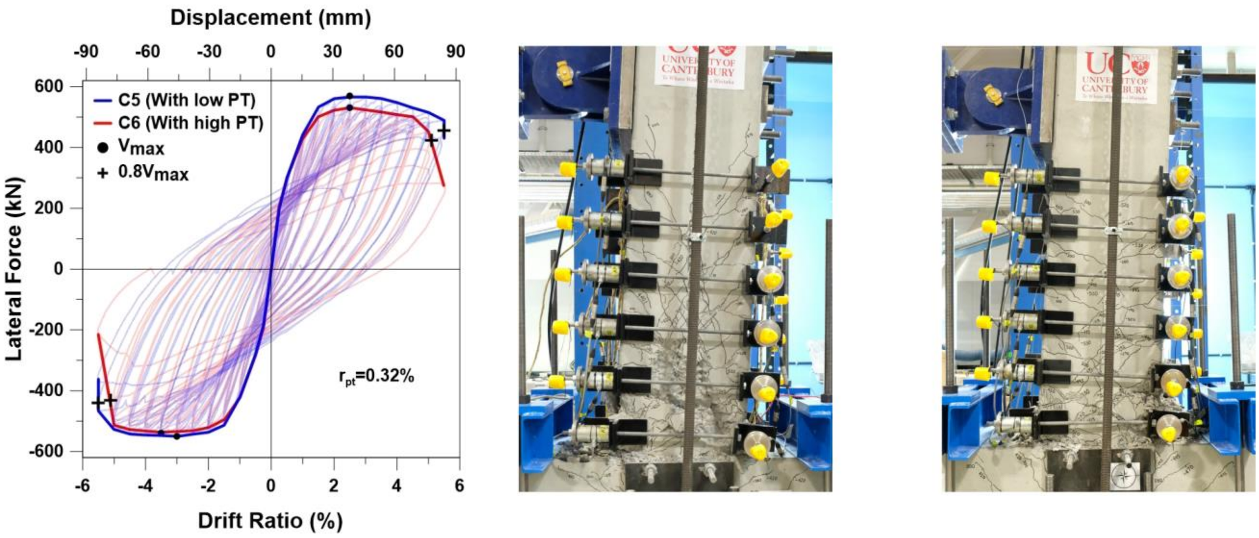

a) *b)* *c)*

Figure 5: a) Hysteretic response of columns C5 and C6; b) Column C5 at a drift ratio of 5.5%; c) Column C6 at a drift ratio of 5.5%

3.2 As a repair measure

Before application of clamps, during stage A of the loading (Fig. 3), damage in columns C10 and C11 consisted in flexural cracks and a critical shear crack. A critical shear crack is defined here as a crack that occurs before flexural cracking in its vicinity. The observed flexural cracks, which were up to 0.45mm thick, occurred in a similar fashion in C10 and C11. The maximum thickness of the critical shear crack in C10 and C11 was measured as 4.0 mm and 1.0 mm, respectively. When such crack was observed, lateral loading was stopped and axial load was removed. Then clamps were mounted and prestressed. Clamping was conducted in less than 4 hours, and columns were tested the day after when was axial load reapplied. Table 3 summarises key test variables and results. Figure 6 shows the hysteretic responses of columns C10 and C11, before repair (Stage A), and after repair (Stage B).

Table 3: Summary of test results on repaired columns

Specimen	Stage	f'_c (MPa)	r_{tr} (%)	s_{pt} (mm)	s_{pt}/d	r_{pt} (%)	σ_L (MPa)	V_{max} (kN)	*D.C.* (%)
C10	A	23	0	-	-	0	-	+300*	0.65**
C10	B	23	0	200	0.7	0.32	1.7	+530/-550	5.3
C11	A	23	0.11	-	-	0	-	+390/-380*	1.0**
C11	B	23	0.11	425	1.0	0.15	0.8	+530/-510	3.7

f'_c: concrete cylinder compressive strength; r_{tr}: reinforcement ratio of conventional ties; s_{pt}: spacing of post-tensioned clamps; *d:* effective depth ratio; r_{pt}: reinforcement ratio of post-tensioned clamps; σ_L: lateral confining stress on the column caused by the clamps; V_{max}: maximum measured shear force; *D.C.*: Drift Capacity.

* Maximum measured force in stage A

** Drift ratio associated with the max. measured force in stage A

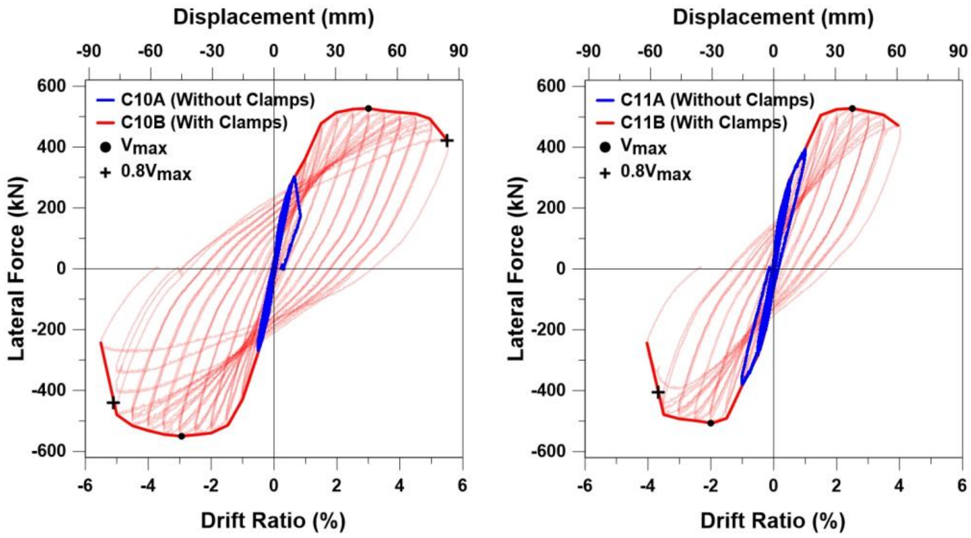

a) *b)*

Figure 6: Hysteretic responses of test columns: a) C10 and b) C11.

For column C10, the first flexural cracks were observed at a lateral load of 120 kN, approximately. The critical shear crack was observed at a load of 300 kN ($v = 1.4$ MPa) and at a drift ratio of 0.65%, approximately. C10 did not have conventional ties, therefore, the measured stress is assumed to be an acceptable approximation to the contribution to shear strength of the concrete v_c (Equation 1). As shown in Figure 7a, the critical shear crack developed along the full height of the column. The specimen was repaired by applying external clamps spaced at 200 mm to each other ($r_{pt} = 0.32\%$) (Fig. 7b). The lateral confining pressure helped to close the critical shear crack, reducing its width from 4.0 mm to 0.5 mm. After repair, the loading protocol was resumed (stage B) as shown in Figure 3. Once repaired, C10 reached flexural yielding of the longitudinal reinforcement at a drift ratio of approximately 1.3%. The existing critical shear crack did not open further and damage was observed in the form of new flexural cracks and flexure-shear cracks. The drift capacity of C10 was 5.3%.

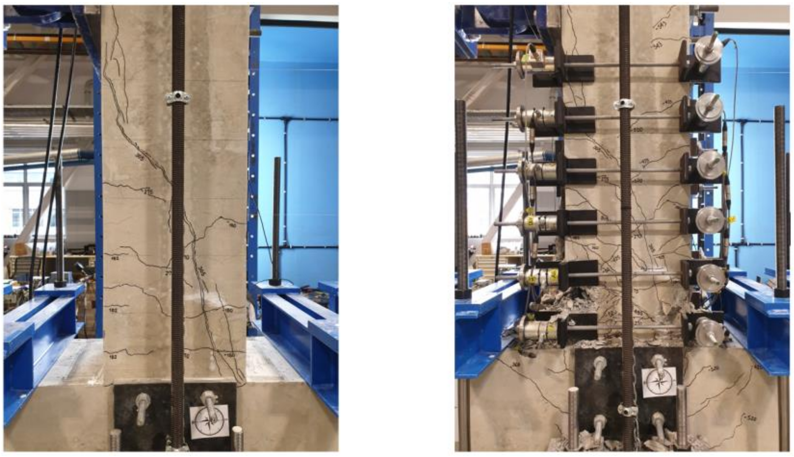

a) *b)*

Figure 7: a) Column C10 - Stage A, b) Column C10 - Stage B

Column C11 had three conventional ties spaced at $d = 425$ mm ($r_{tr} = 0.11\%$). The first one being located at 425 mm from the top face of the foundation. Figure 8a shows the initial damage induced to C11. Inclined shear cracks were observed at 340 kN and -345 kN. The specimen was repaired by applying external clamps spaced at 300 mm to each other ($r_{pt} = 0.21\%$) (Fig. 8b). After repair, C11 reached flexural yielding of the longitudinal reinforcement at a drift ratio of approximately 1.5%. At a drift ratio of approximately 3%, spalling was observed at the base of the column between foundation and the closest clamp. Flexural-shear cracks, forming between clamps roughly at the location of the conventional ties, extended rapidly into the compression zones at the base of the column. The column failed in the first cycle at a drift ratio of 4%. The drift capacity of C11 was 3.7%.

a) *b)*

Figure 8: a) Column C11 - Stage A, b) Column C11 - Stage B

4 CONCLUSIONS

- The effects of the initial lateral prestress on drift capacity was observed to be more relevant in columns with shear strength (Equation 1) similar (within 20% larger) to the expected shear demand at flexural yielding of the longitudinal reinforcement. Comparing column C3 with C9, the lateral prestress in the later, increased the drift capacity from 3% to 4%. The mode of failure changed from shear disintegration in C3 to flexural failure in C9. In contrast, when enough transverse reinforcement is placed to exceed (by more than 50%) that required by flexural yielding, there seem not to be an increase in drift capacity. Nonetheless, fewer and narrower cracks were observed in C6 than in C5, as well as a more ductile failure.
- The lateral pressure caused by the clamps on columns C10 and C11 helped narrow the critical shear crack (as defined in Section 3.2) caused during stage A of the loading protocol. After repair, C10 and C11 reached flexural yielding of the longitudinal reinforcement and failed in a ductile manner with drift capacities of 5.3% and 3.7%, respectively.
- The proposed post-tensioned clamps can be used as an effective technique to retrofit and repair RC columns with insufficient transverse reinforcement. The clamps are easy to fabricate and install, and lend themselves well to rapid repair after earthquakes.

5 ACKNOLEDGEMENT

The authors would like to thank QuakeCoRE (New Zealand Centre for Earthquake Resilience) for the financial support provided for this research project and the University of Canterbury for its support in the form of physical and human resources.

6 REFERENCES

Aboutaha, R. S., Engelhardt, M. D., Jirsa, J. O., & Kreger, M. E. (1999). Rehabilitation of shear critical concrete columns by use of rectangular steel jackets. *ACI Structural Journal*, *96*(1), 68–78. https://doi.org/10.14359/597

Andrawes, B., & Shin, M. (2009). Experimental Investigation of Concrete Columns Wrapped with Shape Memory Alloy Spirals. In *Improving the Seismic Performance of Existing Buildings and Other Structures*. https://doi.org/10.1061/41084(364)76

Burgoyne, C., & Balafas, I. (2007). *Why is frp not a financial success?* https://www.omransanatava.ir/images/pdf/ENG/1-1.pdf

Choi, E., Nam, T.-H., Cho, S.-C., Chung, Y.-S., & Park, T. (2008). The behavior of concrete cylinders confined by shape memory alloy wires. *Smart Materials & Structures*, *17*(6), 065032. https://doi.org/10.1088/0964-1726/17/6/065032

Gamble, W. L., Hawkins, N. M., & Kaspar, I. I. (1996). Seismic retrofitting experience and experiments in Illinois. *Proc., 5th National Workshop on Bridge Research in Progress*, 245–250.

Hanson, R. D., & Degenkolb, H. J. (1969). *The Venezuela Earthquake, July 29, 1967*. American Iron and Steel Institute. https://play.google.com/store/books/details?id=J8A8AAAAIAAJ

Holmes, N., Niall, D., & O'Shea, C. (2015). Active confinement of weakened concrete columns. *Materials and Structures*, *48*(9), 2759–2777. https://doi.org/10.1617/s11527-014-0352-1

Kent, D. C., & Park, R. (1971). Flexural Members with Confined Concrete. *Journal of the Structural Division*, *97*(7), 1969–1990. https://doi.org/10.1061/JSDEAG.0002957

Kyoda, N., Yamakawa, T., Nakada, K., Javadi, P., & Nagahama, A. (2011). Emergency Retrofit for Damaged RC Columns by Fiber Belts Prestressing and Plywoods. In *Advances in FRP Composites in Civil Engineering* (pp. 801–805). https://doi.org/10.1007/978-3-642-17487-2_176

Lew, H. S., & Leyendecker, E. V. (1971). *Engineering Aspects of the 1971 San Fernando Earthquake*. U.S. National Bureau of Standards. https://play.google.com/store/books/details?id=w0FSAAAAMAAJ

Mander, J. B., Priestley, M. J. N., & Park, R. (1988a). Observed stress-strain behavior of confined concrete. *Journal of Structural Engineering* , *114*(8), 1827–1849. https://doi.org/10.1061/(asce)0733-9445(1988)114:8(1827)

Mander, J. B., Priestley, M. J. N., & Park, R. (1988b). Theoretical stress-strain model for confined concrete. *Journal of Structural Engineering* , *114*(8), 1804–1826. https://doi.org/10.1061/(asce)0733-9445(1988)114:8(1804)

Moghaddam, H., Samadi, M., Pilakoutas, K., & Mohebbi, S. (2010). Axial compressive behavior of concrete actively confined by metal strips; part A: experimental study. *Materials and Structures*, *43*(10), 1369–1381. https://doi.org/10.1617/s11527-010-9588-6

Raza, S., Khan, M. K. I., Menegon, S. J., Tsang, H.-H., & Wilson, J. L. (2019). Strengthening and Repair of Reinforced Concrete Columns by Jacketing: State-of-the-Art Review. *Sustainability: Science Practice and Policy*, *11*(11), 3208. https://doi.org/10.3390/su11113208

Richart, F. E. (1927). *An Investigation of Web Stresses in Reinforced Concrete Beams* (No. 166). University of Illinois.

Richart, F. E., Brandtzæg, A., & Brown, R. L. (1928). *A study of the failure of concrete under combined compressive stresses*. http://www.ideals.illinois.edu/handle/2142/4277

Rodriguez, M., & Park, R. (1994). Seismic load tests on reinforced concrete columns strengthened by jacketing. *ACI Structural Journal*, *91*(2), 150–159. https://doi.org/10.14359/4593

Rousakis, T. C., & Tourtouras, I. S. (2014). RC columns of square section – Passive and active confinement with composite ropes. *Composites. Part B, Engineering*, *58*, 573–581. https://doi.org/10.1016/j.compositesb.2013.11.011

Roy, H. E. H., & Sozen, M. A. (1965). Ductility of concrete. *Sociological Perspectives: SP: Official Publication of the Pacific Sociological Association*, *12*, 213–235. https://doi.org/10.14359/16718

Saatcioglu, M., & Yalcin, C. (2003). External prestressing concrete columns for improved seismic shear resistance. *Journal of Structural Engineering (New York, N.Y.)*, *129*(8), 1057–1070. https://doi.org/10.1061/(asce)0733-9445(2003)129:8(1057)

Shin, M., & Andrawes, B. (2014). Parametric Study of RC Bridge Columns Actively Confined with Shape Memory Alloy Spirals under Lateral Cyclic Loading. In *Journal of Bridge Engineering* (Vol. 19, Issue 10, p. 04014040). https://doi.org/10.1061/(asce)be.1943-5592.0000609

Skillen, K. C. (2020). *The Effects of Transverse Reinforcement on the Strength and Deformability of Reinforced Concrete Elements* (S. Pujol, Ed.) [PhD]. https://hammer.figshare.com/articles/thesis/The_Effects_of_Transverse_Reinforcement_on_the_Strength_and_Deformability_of_Reinforced_Concrete_Elements/13377242

Tillotson, E. (1960). The agadir earthquake of February 29. *Nature*, *186*(4720), 199–199. https://doi.org/10.1038/186199a0

Tran, H., Balandraud, X., & Destrebecq, J. F. (2015). Improvement of the mechanical performances of concrete cylinders confined actively or passively by means of SMA wires. *Archives of Civil and Mechanical Engineering*, *15*(1), 292–299. https://doi.org/10.1016/j.acme.2014.04.009

Yamakawa, T., Banazadeh, M., & Fujikawa, S. (2005). Emergency Retrofit of Shear Damaged Extremely Short RC Columns Using Pre-tensioned Aramid Fiber Belts. *Journal of Advanced Concrete Technology*, *3*(1), 95–106. https://doi.org/10.3151/jact.3.95

Yamakawa, T., Kamogawa, S., & Kurashige, M. (2000). Seismic Performance and Design of RC Columns Retrofitted by PC Bar Prestressing as External Hoops. *J. of Structural and Construction Engg., AIJ*, *537*, 107–113. https://ci.nii.ac.jp/naid/10018682035/